Supporting Information

Ross et al. 10.1073/pnas.1008189107

SI Materials and Methods

Animals. Homozygous mtDNA mutator animals and wild-type controls were obtained by intercrossing mice heterozygous for the mtDNA mutator allele (+/PolgA^{mut}) and genotyped as previously described (1). Control strains C57BL/6J and 129/SvImJ mice (JAX Mice Strains) were also used. Among the oldest wild-type mice (130 wk), one animal was excluded because of tumor-like liver inclusions. Mice were fed ad libitum (R70 Standard Diet; Lactamin), had free access to water, and were kept on a 12:12-h light:dark cycle at 24 °C. Experiments were approved by the Animal Ethics Committee of the North Stockholm region and conducted in accordance with international standards on animal welfare. Adequate measures were taken to minimize pain and discomfort.

In regard to the ages at which animals were examined, it was previously determined that mtDNA mutator mice seem to be born healthy, have a life expectancy of ~46–48 wk, and show visible aging phenotypes after 24 wk of age (1). Although the accumulation of mtDNA mutations is random in nature, all mtDNA mutator mice seem to age in a similar manner. Therefore, we typically studied these animals at a young age (9–12 wk) and an old age (42–46 wk) but also tested to combine young and middle ages if we saw no differences between the two age groups. We first conducted a timeline to evaluate lactate levels using proton magnetic resonance spectroscopy (^{1}H-MRS) but could not use animals older than 38 wk of age, because they did not respond well to anesthesia. Because breeding mtDNA mutator mice is difficult and all mtDNA mutator mice examined by ^{1}H-MRS showed elevated lactate levels, we chose a middle age mtDNA mutator mouse group (25–29 wk) to confirm the ^{1}H-MRS findings. On confirmation, we also investigated lactate levels in similarly middle age wild-type controls (86 wk). We also conducted a temporal study of mitochondrial dysfunction in mtDNA mutator mice, and then compared old age mtDNA mutator mice with old age wild-type controls (130 wk). For the in situ hybridization studies of the brain, we used young age and old age mtDNA mutator mice compared with old age wild-type controls. We then used middle age and old age mtDNA mutator mice for in situ hybridization in peripheral tissues and enzymatic characterization.

^{1}H-MRS. ***Animal preparation.*** Animals were anesthetized with 3.5% isoflurane for induction and 2.0% for maintenance with 30% oxygen. Mice were attached in a supine position to an acrylic rig. Body temperature was maintained at 36 ± 0.5 °C with a warm laminar air stream. Heart rate and respiration were monitored, and the percentage of isoflurane was regulated to maintain 80 ± 20 respirations min^{-1}.

Determination of metabolites. ^{1}H-MRS was performed on animals as previously described (2) on a horizontal 4.7 T/40-cm magnet (BioSpec Avance 47/40; Bruker) equipped with a 12-cm inner diameter self-shielded gradient system (maximum gradient strength = 200 mTm^{-1}). A linear birdcage resonator with an inner diameter of 25 mm was used for excitation and detection. Because lactate is mainly affected by chemical shift displacement in the ^{1}H spectrum, minimization of possible spectrum contamination from lipids and macromolecules becomes critical for accurate lactate quantification. Voxel shape and localization was achieved by point-resolved spectroscopy (PRESS) using Hermite radio frequency (RF) pulses with a matched bandwidth (BW) of 5 kHz. To enhance voxel shape definition, outer volume suppression (OVS) was applied using hyperbolic secant pulses with a BW of 20 kHz. As a result, the maximum voxel displacement referenced to lactate was about 10% of the voxel size. The quality of the spectra was further improved by phase cycling of the RF pulses and the receiver in 16 steps (exorcycle), reducing the contribution of unwanted signals arising from nonrefocused coherencies. The chosen short echo time (TE) of 15.9 ms delivers high signal-to-noise ratio (SNR) and does not complicate the spectrum by the development of j-coupled (indirect dipole–dipole coupling) spin–spin systems of lactate. To achieve sufficient accuracy for quantification, a repetition time (TR) of sufficient length (TR = 3,500 ms) was chosen, allowing complete relaxation of most metabolites in the spectrum between consecutive scans. Reliable water suppression was accomplished by applying the variable power RF pulses and optimized relaxation delays (VAPOR) method (3) in three steps. Total length of the water suppression module interleaved with OVS was 700 ms, allowing sufficient water suppression during the time of data acquisition.

Spectra from cerebral cortex and striatum were obtained from volumes of interest (VOI) of 10.2 and 20.0 μL, respectively, with 512 averages and a spectral width of 2 kHz. This resulted in an average SNR of 5 (cerebral cortex) and 10 (striatum) in reference to the creatine peak at 3.03 ppm. The spectral resolution was improved by local shimming at VOI, resulting in a full width at one-half maximum of the water peak of 8–13 Hz. The accurate positioning of the VOI was based on multislice high-resolution anatomical images [fast spin echo/rapid acquisition with relaxation enhancement (RARE)] in axial, sagittal, and coronal planes. The required contrast was achieved by T1/T2 weighting with the following parameters: TR/TE = 2,500/47 ms (echo spacing = 11.7 ms and number of echoes = 8), pixel size = 0.12 × 0.12 mm^2, and slice thickness = 1 mm. In the axial position, the slice package was positioned with the first slice at the rhinal fissure. The VOI in cerebral cortex (4.0 × 1.6 × 1.6 mm = 10.2 μL) was positioned as illustrated in Fig. 1*A*, taking care not to include the subdural space. In striatum, the VOI (5.0 × 2.0 × 2.0 mm = 20.0 μL) was positioned 9.0 mm caudal to the rhinal fissure, illustrated in Fig. S2*A*.

Metabolite quantification. The software package LCModel (http://s-provencher.com) was used for analysis of the spectra (4, 5), and statistics were applied as previously described (2, 6). The quantification algorithm of LCModel applies linear combinations of model spectra to calculate the best fit of the experimental spectrum. The model spectra are calibrated to match magnetic field strength, sequence type, and sequence parameters used for data acquisition. Lactate concentrations were calculated as ratios to the total creatine concentrations (Cr + PCr). This methodology has been used by others (7, 8). Criteria for reliable metabolite quantification were based on the Cramér–Rao lower bounds (CRLB) for each metabolite as well as the CRLB for sum of spectrally overlapping metabolites, which estimates the SD of the model spectra's fit to the experimental data. Metabolites with CRLB less than 50% were considered for further analysis.

HPLC. ***Tissue preparation with blood.*** Animals were killed by cervical dislocation, and tissues including whole brain, liver, and heart were removed within 15–20 s, rapidly frozen in liquid nitrogen for 6 s, powdered over dry ice, and homogenized in 4 mL of 12% (vol/vol) perchloric acid ($HClO_4$) solution (wt/vol) at 0 °C using a polished glass tube pestle homogenizer. Blood was collected from the severed vessels and centrifuged 5 min at 4,000 × *g*, and 1 mL 7% (vol/vol) $HClO_4$ was added to 1 mL plasma. The ho-

mogenates and plasma samples were centrifuged at 40,000 × *g* for 15 min, the supernatants were placed in an ice bath and neutralized to pH 4–5 with potassium hydroxide (KOH), and the pellets were weighed for analysis. Samples were centrifuged for another 15 min at 40,000 × *g* to sediment the precipitant, potassium perchlorate ($KClO_4$), which formed after neutralization with KOH. Supernatants were retained and filtered (0.2 μm) before lyophilization. This protocol is based on an effective procedure to measure lactate levels by Kehr (9).

Tissue preparation with blood removed. For tissue preparation, with blood removed, animals were anesthetized with 40 mg kg^{-1} body weight pentobarbital (10), and arterial blood was collected and lyophilized as described above. Anesthetized animals were perfused with 20 mL Ca^{2+}-free Tyrode's solution, and whole brain, heart, and liver were rapidly removed, frozen, homogenized, and lyophilized as described above.

Determination of lactate. Lactate levels were determined by ion-exchange column liquid chromatography with UV detection. The chromatographic system included a pump (BAS 460; Bioanalytical Systems), a refrigerated microsampler (CMA/200; CMA/Microdialysis), and a UV detector (BAS 116, operating at 214 nm; Bioanalytical Systems). Chromatograms were recorded and integrated by use of a computerized data acquisition system (DataApex). Lactate was separated on a 250 × 4.6 internal diameter mm Polypore H column (Bioanalytical Systems). The mobile phase consisted of 2.5 mM sulphuric acid pumped at a flow rate of 0.3 mL/min. Lactate levels were expressed as mmol L^{-1} for plasma and μmol g^{-1} for tissue samples.

Tissue Preparation for Cryosectioning. For preparation of fresh frozen sections for histochemistry and in situ hybridization, animals were killed by cervical dislocation; brain, heart, and liver were rapidly frozen on dry ice and stored in −80 °C. Frozen tissues were embedded (Tissue-Tek; Sakura Finetek), and 14-μm cryostat (Microm Model HM 500M Cryostat; Microm) sections taken at −21 °C were thawed onto slides (Super Frost; Menzel-Gläser) and stored at −20 °C until use.

Enzyme Histochemistry. To visualize respiratory dysfunction, we used enzyme histochemistry to determine the activities of COX and succinate dehydrogenase (SDH) (11). COX, or complex IV, is a respiratory chain enzyme with critical components encoded by mtDNA. SDH, or complex II, is the only enzyme to participate in both the citric acid cycle and the mitochondrial electron transport chain. It is entirely encoded by nuclear DNA. Impaired expression of mtDNA typically leads to a pattern of severe reduction in complex IV activity and preserved complex II activity. Respiratory chain-deficient cells will stain blue with the COX/SDH double histochemistry method, whereas cells with normal respiratory chain function will appear dark brown. COX/SDH histochemistry was performed on coronal 14-μm cryostat sections at hippocampal and striatal levels as described earlier (12). Frozen sections were air dried for 1 h. Sections were then incubated for 40 min at 37 °C with 3,3′-diaminobenzidine tetrahydrochloride (Sigma Liquid Substrate System D7304; Sigma), 500 μM cytochrome *c*, and bovine catalase. The sections were then washed four times at 10 min in 0.1 M PBS (pH 7.0). Next, 1.875 mM nitroblue tetrazolium (NBT), 1.30 M sodium succinate, 2.0 mM phenazine methosulfate (PMS), and 100 mM sodium azide were applied to the sections for 40 min at 37 °C. Sections were then washed, dehydrated in increasing concentrations of ethanol (70%, 95%, and 99.5%), coverslipped, and visualized under brightfield microscopy. To determine mitochondrial dysfunction indicated by blue staining, slides were coded, and key brain regions were semiquantified for amount of blue stain on a blind basis using a scale of 0–4 (0, no blue staining; 4, only blue staining). Semiquantification was performed bilaterally in cerebral cortex, hippocampus, nucleus accumbens, striatum, and thalamus, and mean values were calculated for each area and animal.

Lactate Dehydrogenase Gene (LDH)-A and LDH-B Gene Expression.

Oligonucleotide probes. DNA oligonucleotide probes were used for quantitative in situ hybridization (ISH) to detect levels of mRNA transcripts in defined brain regions and elsewhere. The accuracy of quantitative ISH has been verified by quantitiative PCR (13). Synthetic oligonucleotide probes were ∼50 bp long and had a guanine-cytosine (GC) content of 45%. Mfold web server software (version 3.2) was used to estimate the folding energy (14). Probe specificity was confirmed by first aligning the probe against all publicly known sequences (www.ncbi.nlm.nih.gov/BLAST) and then, cross-referencing the expression with published results from immunohistochemistry, in situ hybridization, and Northern blots. Based on these specificity criteria, two oligonucleotide DNA probes (Thermo Scientific) were designed and tested per gene, all of which worked, and one probe per gene was selected for mRNA quantization: LDH-A: 5′-CACAGGGG TAATCGAAGCCTGCAGTTGGCAGTGTGTCTCAGAGAC-AGT-3′; LDH-B: 5′-GCTTGA TGACTTCATAGGCACTGTC-CACCACCATCTTATGCACCTCCTTCC-3′. Additionally, a random probe with similar sequence length and GC content was used as a negative control, and consecutive sections from a wild-type littermate were inserted as a positive control in each experiment.

ISH. High-stringency radioactive ISH was performed on brain, heart, and liver sections based on the protocol established by Dagerlind et al. (15) to determine mRNA levels. Probes were labeled with α-^{33}P-deoxyadenosine 5′-triphosphate (dATP) at the 3′ end (Perkin-Elmer) using terminal deoxynucleotidyl transferase (TdT) (Amersham Biosciences). Cryosections were air-dried and hybridized overnight at 42 °C with a mixture containing 4× SSC solution (3.0 M trisodium citrate and 3.0 M sodium chloride; pH 7.0), 50% formamide ($HCONH_2$), 1× Denhardt's solution (Ficoll, Polyvinylpyrrolidone, and BSA), 1% sarcosyl, 0.02 M sodium phosphate (Na_3PO_4), 10% dextran sulfate (wt/vol), 0.2 M DTT ($C_4H_{10}O_2S_2$), 0.5 μg μL^{-1} sheared salmon serum sperm DNA, and the radio-labeled oligonucleotide. The next day, slides were washed in 60 °C 1× SSC buffer for 1 h and cooled to room temperature, followed by rapid dehydration in increasing concentrations of ethanol (70%, 95%, and 99.5%) and finally, air-drying. Visualization and quantification of mRNA content in sections were performed and expressed as nCi g^{-1}, as described earlier (16). Slides were exposed first to phosphoimaging plates (Fujix BAS-3000; Fuji Photo Film Co. Ltd.) for qualitative assurance and to determine appropriate film exposure time, and then to autoradiographic films (Biomax; Eastman Kodak) together with ^{14}C standards (Amersham) for 2–5 d, depending on the signal intensity of the radio-labeled oligonucleotide. To determine mRNA content, autoradiographic films were digitized, and mRNA signal intensity was quantified (ImageJ, version 1.38, http://rsb.info.nih.gov/ij/). Optical density readings from scanned autoradiographs were converted to nCi g^{-1} as determined from a ^{14}C-step standard curve. Measurements of optical density from the autoradiographic films were made bilaterally in cerebral cortex and CA1 of hippocampus, and a mean value was calculated for each area and animal.

Microscopy. Brightfield microscopy was used to evaluate results and document enzyme histochemistry results (Zeiss Axiophot 2 and Axioplan 2 Imaging Software, Zeiss Axiophot 2; Carl Zeiss).

Tissue Preparation for Enzymatic Characterization. For preparation of tissue samples used to characterize LDH isoenzymes and enzymatic activity, animals were killed by cervical dislocation, the brains were quickly removed (within 15–20 s) and rinsed in 0.1 M PBS (pH 7.4), after which cerebral cortex was dissected within 5–10 s, rapidly frozen on dry ice, and stored in −80 °C. Tissue

samples were homogenized in 100 mM potassium phosphate buffer (PPB; pH 7.0) with 2 mM g^{-1} tissue of EDTA. Homogenates were centrifuged at 10,000 × *g* for 15 min at 4 °C, and the supernatants were collected for assays.

Measurement of Protein Concentration. Protein concentration was measured in a colorimetric reaction using a protein assay kit (#500–0111; Bio-Rad) according to the manufacturer's instructions. A tunable microplate reader (VERSAmax; Molecular Devices) at 25 °C with absorbance at 750 nm was used, and concentrations were expressed as mg mL^{-1} determined by a BSA standard curve using appropriate software (SoftMax Pro).

LDH Isoenzyme Characterization. Native gel electrophoresis was used to separate and characterize the five known LDH isoenzymes in cerebral cortex using a published protocol (17) based on the procedure of Nissen and Schousboe (18). This assay allows for direct visualization of expressed LDH isoenzymes in their native state. This is not achievable using Western blot or immunohistochemistry. Samples (50-μg protein) were loaded into a 1.5% agarose gel in 25 mM Tris·HCl and 250 mM glycine (pH 9.5) buffer, with a 6× gel-loading buffer consisting of 0.1% bromophenol blue, 15% glycerol, and 20 mM Tris·HCl (pH 8.0). Electrophoresis was conducted for 75 min at 150 V in a 5 mM Tris·HCl and 40 mM glycine (pH 9.5) running buffer. Gels were then washed briefly in 100 mM Tris·HCl (pH 8.5) buffer. To visualize LDH isoenzyme bands, the gel was incubated for 20 min at 37 °C in a solution containing lactate (3.24 mg mL^{-1}), β-nicotinamide adenine dinucleotide (NAD+; 0.3 mg mL^{-1}), NBT (0.8 mg mL^{-1}), and PMS (0.167 mg mL^{-1}) dissolved in 10 mM Tris·HCl (pH 8.5) buffer. LDH isoenzyme concentration was quantified (BioRad) and expressed as percent isoform.

LDH Activity. Spectrophotometric assays were used to determine LDH activity converting pyruvate (P) → lactate (L) as well as L → P in cerebral cortex, detected using a tunable microplate reader (VERSAmax; Molecular Devices) and appropriate software (SoftMax Pro). For $LDH_{L\rightarrow P}$ activity determination, an LDH kit (BioAssay Systems) was used according to the manufacturer's directions. LDH activity in tissue samples was detected at 25 °C with absorbance at 565 nm. For $LDH_{P\rightarrow L}$ activity determination, an assay was designed based on the procedure of Krieg et al. (19). Tissue samples were diluted to 0.05 mg mL^{-1} in 500 mM PPB (pH 7.5) and added to the LDH assay reagent containing 100 mM pyruvate and β-nicotinamide adenine dinucleotide NADH (5 mg/20 mL of assay buffer) in 500 mM PPB at pH 7.5. The change in NADH absorbance was measured at 25 °C in 1-min intervals for 5 min at 340-nm absorbance. LDH activity data were calculated in IU mg^{-1} protein and were expressed as P:L ratio ($LDH_{P\rightarrow L}$/$LDH_{L\rightarrow P}$) and percent change in LDH activity.

Statistical Analysis. Data are presented to three significant digits as mean values (M) or as percent changes with SEM or SD. Statistical analyses were performed using a linear regression model, two-tailed unpaired *t* test, one-way Kruskal–Wallis ANOVA, or two-way between subjects ANOVA using Bonferroni posthoc analysis to evaluate pair-wise differences, with an α level of 0.05. Significances from posthoc and unpaired *t* tests are denoted in figures with $^{*}P < 0.05$, $^{**}P < 0.01$, and $^{***}P < 0.001$, respectively. Statistics were performed using appropriate software (GraphPad Prizm v. 3.02; GraphPad Software Inc).

1. Trifunovic A, et al. (2004) Premature ageing in mice expressing defective mitochondrial DNA polymerase. *Nature* 429:417–423.
2. Westman E, et al. (2009) In vivo 1H-magnetic resonance spectroscopy can detect metabolic changes in APP/PS1 mice after donepezil treatment. *BMC Neurosci* 10:33.
3. Tkác I, Starcuk Z, Choi IY, Gruetter R (1999) In vivo 1H NMR spectroscopy of rat brain at 1 ms echo time. *Magn Reson Med* 41:649–656.
4. Provencher SW (1993) Estimation of metabolite concentrations from localized in vivo proton NMR spectra. *Magn Reson Med* 30:672–679.
5. Provencher SW (2001) Automatic quantitation of localized in vivo 1H spectra with LCModel. *NMR Biomed* 14:260–264.
6. Oberg J, et al. (2008) Age related changes in brain metabolites observed by 1H MRS in APP/PS1 mice. *Neurobiol Aging* 29:1423–1433.
7. Ackl N, et al. (2005) Hippocampal metabolic abnormalities in mild cognitive impairment and Alzheimer's disease. *Neurosci Lett* 384:23–28.
8. Frederick BD, et al. (2004) In vivo proton magnetic resonance spectroscopy of the temporal lobe in Alzheimer's disease. *Prog Neuropsychopharmacol Biol Psychiatry* 28:1313–1322.
9. Kehr J (1999) *Modern Techniques in Neuroscience Research*, eds Windhorst U, Johansson H (Springer, Heidelberg), pp 1149–1198.
10. Taber R, Irwin S (1969) Anesthesia in the mouse. *Fed Proc* 28:1528–1532.
11. Seligman AM, Karnovsky MJ, Wasserkrug HL, Hanker JS (1968) Nondroplet ultrastructural demonstration of cytochrome oxidase activity with a polymerizing osmiophilic reagent, diaminobenzidine (DAB). *J Cell Biol* 38:1–14.
12. Larsson NG, et al. (1998) Mitochondrial transcription factor A is necessary for mtDNA maintenance and embryogenesis in mice. *Nat Genet* 18:231–236.
13. Broide RS, et al. (2004) Standardized quantitative in situ hybridization using radioactive oligonucleotide probes for detecting relative levels of mRNA transcripts verified by real-time PCR. *Brain Res* 1000:211–222.
14. Mathews DH, Burkard ME, Freier SM, Wyatt JR, Turner DH (1999) Predicting oligonucleotide affinity to nucleic acid targets. *RNA* 5:1458–1469.
15. Dagerlind A, Friberg K, Bean AJ, Hökfelt T (1992) Sensitive mRNA detection using unfixed tissue: Combined radioactive and non-radioactive in situ hybridization histochemistry. *Histochemistry* 98:39–49.
16. Westerlund M, et al. (2008) Developmental regulation of leucine-rich repeat kinase 1 and 2 expression in the brain and other rodent and human organs: Implications for Parkinson's disease. *Neuroscience* 152:429–436.
17. Acosta ML, et al. (2005) Early markers of retinal degeneration in rd/rd mice. *Mol Vis* 11:717–728.
18. Nissen C, Schousboe A (1979) Activity and isoenzyme pattern of lactate dehydrogenase in astroblasts cultured from brains of newborn mice. *J Neurochem* 32:1787–1792.
19. Krieg AF, Rosenblum LJ, Henry JB (1967) Lactate dehydrogenase isoenzymes a comparison of pyruvate-to-lactate and lactate-to-pyruvate assays. *Clin Chem* 13:196–203.

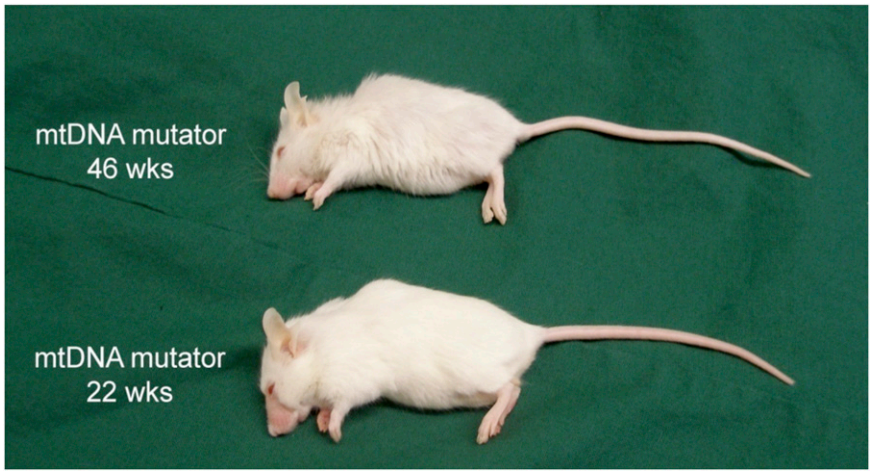

Fig. S1. Examples of mtDNA mutator mice at 22 and 46 wk showing progression of the premature aging phenotype. As mtDNA mutator mice age, there are visible signs of aging, such as alopecia, kyphosis, reduction in body size, and weight loss.

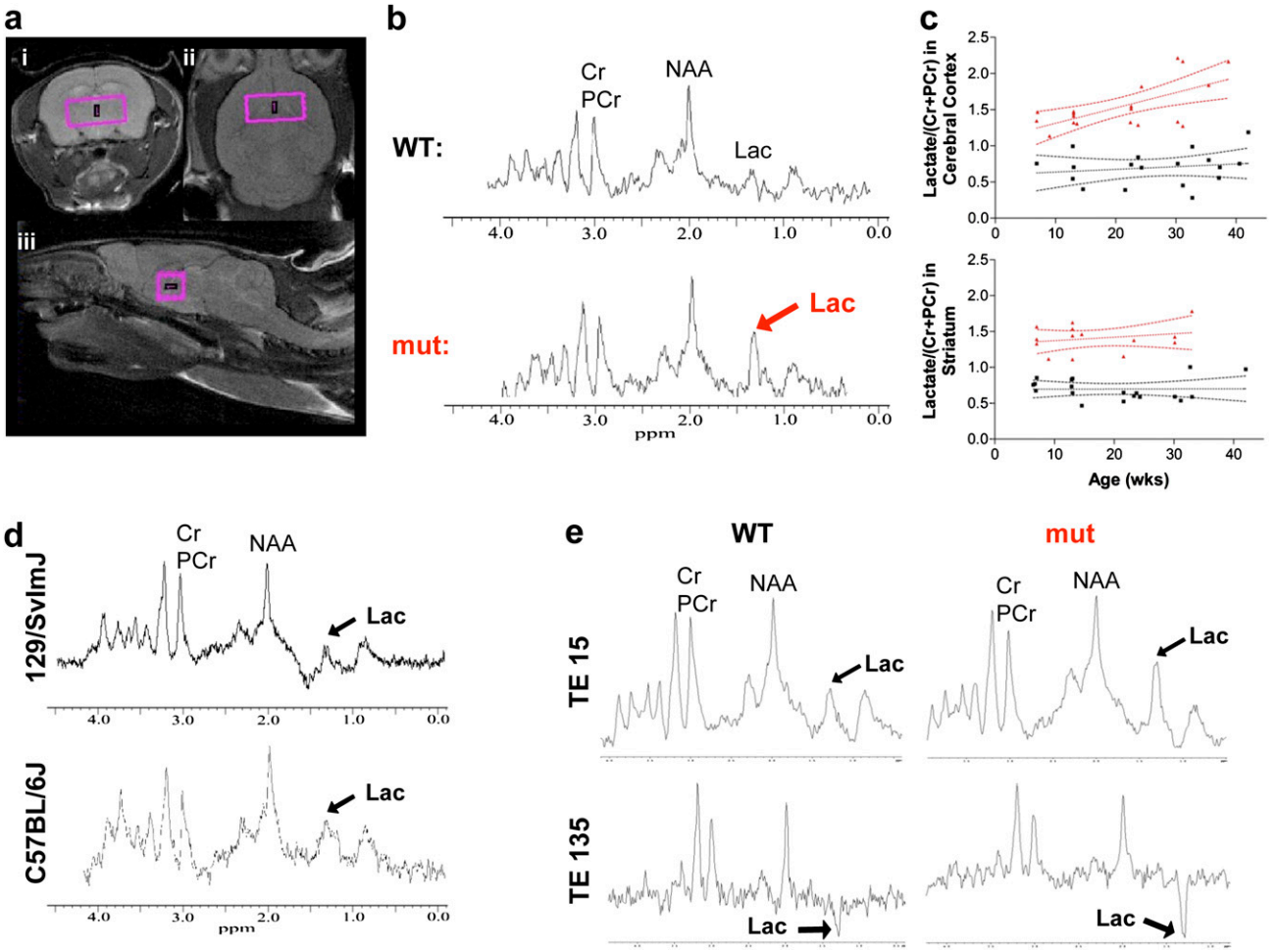

Fig. S2. (*A*) Position of the volume of interest (VOI) in striatum in (*i*) axial, (*ii*) coronal, and (*iii*) sagittal planes. (*B*) Typical proton magnetic resonance (MR) spectra obtained from a VOI in striatum, indicating the marked increase in the lactate doublet (centered on 1.33 ppm) in mtDNA mutator mice. (*C*) Linear regression analysis was performed on brain lactate concentrations in cerebral cortex and striatum from mtDNA mutator (n = 19; red) and littermate wild-type (n = 18; black) mice. In cerebral cortex, lactate levels increased over a 32-wk period by 2.1%/wk [r^2 = 0.404; $F(17)$ = 11.5; P = 0.003], leading to threefold higher levels in mtDNA mutator mice at 35–38 wk. In striatum, lactate levels did not significantly increase as mtDNA mutator mice aged [r^2 = 0.053; $F(12)$ = 0.666; P = 0.430]. (*D*) To exclude the possibility that the genetic background of mutator mice could contribute to the high cerebral lactate levels, we also performed ^{1}H-MRS in 129/SvImJ and C57BL/6J mice. Typical proton MR spectra obtained from a VOI in striatum of 129/SvImJ and C57BL/6J mice averaged from 512 scans are shown. The spectra show the presence of the lactate doublet (centered on 1.33 ppm) similar to the peak observed in wild-type littermates of mtDNA mutator mice. (*E*) Proton MR spectra obtained from a VOI in striatum from an mtDNA mutator and a wild-type littermate mouse with a short echo time (TE) of 15 ms show the lactate peak above the baseline. To ensure that an increase in the lactate peak was not confounded by partly overlapping peaks, as can be the case with lactate and overlapping lipids and lipid-like with macromolecules, a long TE of 135 ms was also used to minimize potential contamination. With the long TE, the characteristic phase inversion of the doublet peak to below baseline occurred and revealed an increase in the lactate peak in the mtDNA mutator mouse spectrum, similar to that shown with the shorter TE. This suggests that the amount of lactate in mtDNA mutator mice is sufficient to enable LCModel to resolve lactate confidently from overlapping lipid and lipid-type macromolecules.

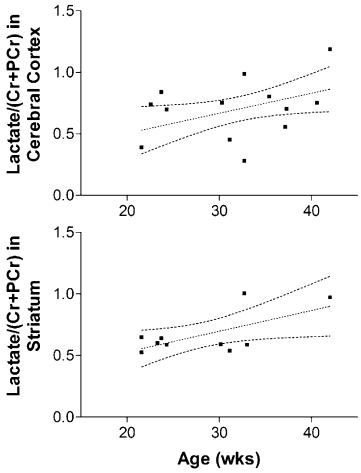

Fig. S3. Linear regression analysis of brain lactate concentrations from wild-type control mice in cerebral cortex (n = 13) and striatum (n = 10) from 20 to 42 wk of age. Lactate levels increased over the 22-wk period in cerebral cortex by 1.6%/wk [r^2 = 0.1852; $F(11)$ = 4.773; P = 0.040] and striatum by 1.7%/wk [r^2 = 0.418; $F(8)$ = 5.746; P = 0.043). Lactate levels from 20 wk of age and older were analyzed, because the earliest age at which wild-type mice showed mitochondrial dysfunction was 36–37 wk of age (Fig. 2*B*).